Iris Recognition using Consistent Corner Optical Flow

Aditya Nigam and Phalguni Gupta

Department of Computer Science and Engineering,
Indian Institute of Technology Kanpur, India-208016
{naditya,pg}@cse.iitk.ac.in

Abstract. This paper proposes an efficient iris based authentication system. Iris segmentation is done using an improved circular hough transform and robust integro-differential operator to detect inner and outer iris boundary respectively. The segmented iris is normalized to polar coordinates and preprocessed using $LGBP$ (Local Gradient Binary Pattern). The corners features are extracted and matched using dissimilarity measure $CIOF$ (Corners having Inconsistent Optical Flow). The proposed approach has been tested on publicly available CASIA 4.0 Interval and Lamp databases consisting of $2,639$ and $16,212$ images respectively. It has been observed that the segmentation accuracy of more than 99.6% can be achieved on both databases. This paper also provides error classification for wrong segmentation and also determines influential parameters for errors. The proposed system has performed with CRR of 99.75% and 99.87% with an EER of 0.108% and 1.29% on Interval and Lamp databases respectively.

1 Introduction

Biometrics can be an alternative to any token-based as well as knowledge based traditional methods as they are easier to use and harder to circumvent. The state of the art identification systems are mainly based on fingerprint, face [16, 17], iris [5, 22, 21, 2, 12, 14] and palmprint as major biometric traits along with some minor traits such as finger-knuckle [18], gait *etc.* But each biometric trait has its own set of challenges and trait specific issues. Thin circular diaphragm between cornea and lens is called as iris which have abundance of micro-textures as crypts, furrows, ridges, corona, freckles and pigment spots. These textures are randomly distributed; hence they are believed to be unique [10]. Iris texture is stable between subjects and even between right and left eye of the same subject [7]. Iris is a well-protected biometric trait as compared to the other traits and it is also invariant to age.

Huge amount of work is done in the field of iris recognition. In [5], gabor wavelet responses are quantized to generate feature vector and matching is done using hamming distance. In [22], hough transform is used for iris localization and Laplacian of Gaussian (LOG) is used for matching. In [12], vanishing and appearing of important image structures are considered as key local variations and dyadic wavelets are used to transform 2D image signals into 1D signals for unique features. There are some significant contributions like application of Principle Component Analysis (PCA) and Independent Component Analysis (ICA) on iris recognition in [4, 9]. In [8], gabor wavelet with elastic graph matching is used for iris recognition. In [15], Discrete Cosine Transform (DCT) coefficients are quantized that are extracted from non-overlapping rectangular angular blocks and matched using hamming distances. In [14], phase only correlation (POC) and band limited phase only correlation ($BLPOC$) are used for accurate iris recognition. In [21], compact and highly efficient ordinal measures are applied for iris recognition. In [19], variational model is applied to localize iris while modified contribution selection algorithm ($MCSA$) is used for iris feature ranking. A comprehensive iris literature survey is presented in [3].

Iris recognition systems consist of several steps: *Image acquisition*, *Iris Segmentation*, *Iris Normalization*, *Preprocessing*, *Feature extraction* and *Matching*. Each step affects overall performance of the system, but segmentation is the most critical step. Wrong segmentation would render the subsequent steps meaningless. In this paper some new steps are proposed in iris segmentation making it efficient and accurate followed by a novel iris enhancement, transformation and recognition method. The paper is organized as follows: Section 2 describes the proposed system. Section 3 presents the experimental results followed by the last section that presents the concluding remarks.

2 Proposed System

In this paper two state of the art techniques (Integro-differential and Hough transformation) are applied in a way such that they can compliment each other for efficient and accurate iris segmentation. The iris texture is enhanced by the proposed local enhancement method. A novel $LGBP$ transformation (*i.e. Local Gradient Binary Pattern*) that uses x and y direction gradient information is proposed to get robust image information representation (*i.e. vcode* and *hcode*). Corner Features are extracted from *vcode* and *hcode* by calculating the eigen values of Hessian matrix at every pixel. Iris recognition is performed by tracking corner features in the corresponding *vcode* and *hcode* considering the consistent optical flow and using $CIOF$ (*i.e. Corners having Inconsistent Optical Flow*) dissimilarity measure.

2.1 Iris Segmentation

The proposed iris segmentation approach involves two major steps: (A) Inner boundary localization followed by (B) Outer boundary localization of iris images.

[A] Inner boundary localization: An iris image I is first *thresholded* to filter out the dark pupil pixels. The resultant binary image is *flood-filled* to remove specular reflection, so that it does not affect the boundary detection as shown in Fig. 1(b). For inner boundary detection strong edges are detected by applying vertical and horizontal Sobel filters.

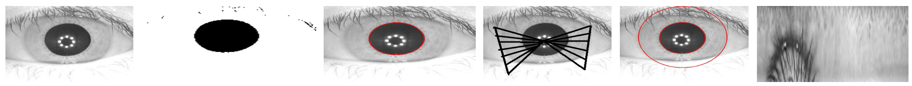

(a) Original (b) Thresholded (c) Seg. Pupil (d) Angle (e) Seg. Iris (f) Nor. Iris

Fig. 1. Automatic Iris Segmentation

Standard hough transform extracts circle in an image by searching the optimal parameters in the whole three dimensional parametric space of abscissa and ordinate of center and radius *i.e* 3-tuple $< x, y, r >$. It has been improved by using the orientation of each pixel to reduce the search space from $3D$ to $1D$ of the radius only. The improved Hough transform can efficiently detect the circle without reducing the accuracy as shown in Fig. 1(c). It makes use of the key observation that "*if an edge point lies on a circle, then the center of circle should lie on the normal to the edge direction (orientation) at that point*". Thus, for an edge point (x, y) in an image and for a radius r, the center coordinates (c_1^x, c_1^y) and (c_2^x, c_2^y), for two circles (one to its left and other to right half) can be computed as:

$$(c_1^x, c_1^y) = (x + r \cdot \sin\left(\theta(x,y) - \frac{\pi}{2}\right), \quad y - r \cdot \cos\left(\theta(x,y) - \frac{\pi}{2}\right)) \tag{1}$$

$$(c_2^x, c_2^y) = (x - r \cdot \sin\left(\theta(x,y) - \frac{\pi}{2}\right), \quad y + r \cdot \cos\left(\theta(x,y) - \frac{\pi}{2}\right)) \tag{2}$$

[B] Outer boundary localization: The robust circular integro-differential operator as defined in [6], is applied over two non-occluded sectors which are selected empirically. Inner boundary localization of iris is used to guide the outer boundary localization. A simple heuristic which is used to make process efficient is that "*iris inner and outer boundaries have centers which are not necessarily concentric, but within a certain small window (W) of each other*". Thus, candidate center points of outer boundary are generated within a window of the inner center. Each of these candidates (c^x, c^y) and radius r defines a circle for the the outer iris boundary. The standard integro-differential operator sums the pixel intensity values over this circle and calculates the change in the summation over a neighbor concentric circle. The candidate circle with the maximum change per unit circumference gives the outer iris boundary. To prevent noise due to eyelids and lashes the circular summation is done over empirically selected two non-occluded sectors of α_{range}=$(-\pi/4, \pi/6)^c \cup (5\pi/6, 5\pi/4)^c$ as shown in Fig. 1(d). Finally segmented iris image is shown in Fig. 1(e).

2.2 Iris Normalization

After iris is segmented from the image, it is transformed to polar coordinates in order to overcome the dimensional inconsistencies between eye images as suggested in [6]. In this paper, the segmented iris images are unwrapped into normalized images of 40×256 size as shown in Fig. 1(f).

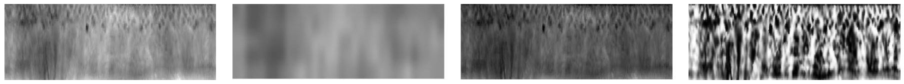

(a) Original Iris (b) Estimated Illum. (c) Uniform Illum. (d) Weiner Filtering

Fig. 2. Iris Texture Enhancement

2.3 Iris Recognition

The texture of normalized iris images are enhanced and transformed to robust representation *i.e vcode, hcode* that can tolerate illumination variations. To achieve some robustness against affine transformations KL-tracking, that is constrained by some statistical and geometrical parameters is used for matching.

[A] Iris Enhancement: The texture of unwrapped iris images are enhanced so as to make the information more discriminative using the proposed local enhancement method. The iris image is divided into blocks of size 8×8 and the mean of these blocks are considered as the coarse illumination of that block. This mean is expanded to the original size of the iris as shown in Fig. 2(b). Smaller block size produces almost same estimate of illumination as that of the original image and bigger will produce improper estimates. Non-uniform illumination is compensated by subtracting estimated illumination from the original image to obtain uniformly illuminated iris image as shown in Fig. 2(c). Then the contrast of uniformly illuminated image is enhanced using Contrast Limited Adaptive Histogram Equalization (CLAHE). It removes the artificially induced borders of tiles using bilinear interpolation and enhances the contrast of image without introducing any external noise. Finally, wiener filter is applied for reducing constant power additive noise to obtain enhanced texture iris image as shown in Fig. 2(d). It can be observed that the texture of enhanced image Fig. 2(d) is much better than Fig. 2(a). The proposed enhancement method has shown encouraging recognition performance boost-up as discussed in Section 3.2 and shown in Fig. 6(a).

[B] *LGBP* Transformation: It transforms normalized and enhanced noisy iris images into *vcode* and *hcode* respectively so as to obtain robust features. The gradient of any edge pixel will be positive if it lies on an edge created due to light to dark shade (*i.e. high to low gray value*) transition else it will be having negative gradient value. Hence all the edge pixels can be divided into two classes of $+ve$ and $-ve$ gradient values as shown in Fig. 3. The *sobel* kernel lacks rotational symmetry hence more consistent *scharr* kernels which are obtained by minimizing angular error is applied. The *scharr* x-direction kernel of size 3×3 and 9×9 are applied to get Fig. 3(b), 3(c) respectively. Bigger size kernel produces coarse level features as shown in Fig. 3(c). This gradient augmented information of each edge pixel can be more discriminative and robust. The proposed transformation precisely uses this information to calculates a 8-bit code for each pixel using x and y-direction derivatives of its 8 neighboring pixels to obtain *vcode* and *hcode* respectively.

(a) Original (b) Transformed (kernal=3) (c) Transformed (kernal=9)

Fig. 3. $LGBP$ Transformation (Red: -ve gradient;Green: +ve grad.;Blue: zero grad.)

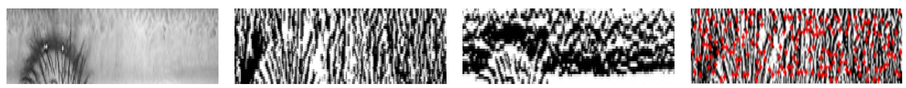

(a) Unwrapped Iris (b) *vcode* (c) *hcode* (d) *vcode* Corners

Fig. 4. Iris Recognition Steps

Let $P_{i,j}$ be the $(i,j)^{th}$ pixel of an iris image P and $Neigh[l], l = 1, 2, ...8$ are the gradients of 8 neighboring pixels centered at pixel $P_{i,j}$ obtained by applying *scharr* kernel, then the k^{th} bit of the 8-bit code (termed as *lgbp_code*) is given by

$$lgbp\_code[k] = \begin{cases} 1 & \textbf{if} \ \ Neigh[k] > 0 \\ \\ 0 & \textbf{otherwise} \end{cases} \tag{3}$$

In *vcode* or *hcode* every pixel is represented by its *lgbp_code* as shown in Fig. 4(b), 4(c) respectively. The pattern of edges within a neighborhood can be assumed to be robust; hence each pixel's *lgbp_code* is considered which is just an encoding of edge pattern in its 8-neighborhood. Also *lgbp_code* of any pixel considers only the sign of the derivative within its specified neighborhood hence ensures the robustness of the proposed transformation in illumination variation.

[C] Feature Extraction Using KLT Corner Detector [20]: Corners in *vcode* and *hcode* are robust features that can be tracked accurately even in varying illumination because they have two high derivatives in orthogonal directions. The eigen analysis of Hessian matrix of size 2×2, for each pixel is done and two possible eigen values λ_1 and λ_2 such that $\lambda_1 \geq \lambda_2$ are obtained. Like [20], all pixels having $\lambda_2 \geq T$ (smaller eigen value greater than a threshold) are considered as corner feature points as shown in Fig. 4(d).

[D] Matching Using KL Tracking [11]: Let $Iris_a$ and $Iris_b$ are two normalized enhanced iris images that have to be matched and I_A^v, I_B^v and I_A^h, I_B^h are their corresponding *vcode* and *hcode* respectively. KL tracking [11] has been used for matching between $Iris_a$ and $Iris_b$. It is assumed that the tracking performance of KL algorithm is good while tracking between features of same subject (genuine matching) and degrades substantially for others (imposter matching).

KL Tracking [11]: Let us assume a corner at spatial location (x, y) in an image I with intensity $I(x, y, t)$ at some time instance t. KL Tracking can be used to estimate sparse optical flow at time instance $t + \delta t$. This estimate is based on three assumptions; [1] Brightness consistency, [2] Temporal persistence and [3] Spatial coherency as defined below:

[1] Brightness Consistency: It assumes little change in brightness for the small value of δt.

$$I(x, y, t) \approx I(x + \delta x, y + \delta y, t + \delta t) \tag{4}$$

[2] Temporal Persistence: Small feature movement for small δt. One can get Eq. (5) for each corner feature.

$$I_x V_x + I_y V_y = -I_t \tag{5}$$

where V_x, V_y are the respective components of the optical flow velocity for feature at pixel $I(x, y, t)$ and I_x, I_y and I_t are the local image derivatives in x, y and t directions respectively.

[3] Spatial Coherency: Estimating unique flow vector from Eq. (5) for every feature point is an ill-posed problem. Hence KL tracking estimates the motion of any feature by assuming local constant flow (*i.e* a patch of pixels moves coherently).

The tracking performance depends on how well these three assumptions are satisfied. However, all tracked corner features may not be the true matches because of noise, local non-rigid distortions in iris and also less difference in inter class and more in intra class matching.

Consistent Optical Flow: It can be noted that true matches have the optical flow which can be aligned with the actual affine transformation between the two images. The estimated optical flow direction is quantized into eight directions and the most consistent direction is selected as the one which has most number of successfully tracked corner features. Any corner matching having optical flow direction other than the most consistent direction is considered as false matching. A dissimilarity measure $CIOF$ (Corners having Inconsistent Optical Flow) has been proposed to estimate the KL-tracking performance by evaluating some geometric and statistical quantities that are defined as:

[a] Proximity Constraints: Euclidean distance between any corner and its estimated tracked location should be less than or equal to an empirically selected threshold TH_d. The parameter TH_d depends upon the amount of translation and rotation in the sample images. High TH_d signifies more translation and vise-versa.

[b] Patch Dissimilarity: Tracking error defined as pixel-wise sum of absolute difference between a local patch centered at current corner and that of its estimated tracked location patch should be less than or equal to an empirically selected threshold TH_e. The parameter TH_e ensures that the matching corners must have similar neighboring patch around it.

Matching Algorithm: Given two *vcode* I_A^v, I_B^v and two *hcode* I_A^h, I_B^h, Algorithm 1 has been presented which can be used to compare $Iris_a$ with $Iris_b$ using $CIOF$. The *vcode* I_A^v, I_B^v are matched while *hcode* I_A^h, I_B^h are matched. Final score $CIOF(Iris_a, Iris_b)$ is obtained by using sum rule fusion of horizontal and vertical matching scores. Such a fusion is very useful and boost-up the

Algorithm 1 $CIOF(Iris_a, Iris_b)$

Require: The two *vcode* I_A^v,I_B^v and two *hcode* I_A^h,I_B^h of normalized and enhanced iris images $Iris_a, Iris_b$ respectively.
N_a^v, N_b^v,N_a^h and N_b^h are the number of corners in I_A^v, I_B^v, I_A^h, and I_B^h respectively.

Ensure: Return the symmetric function $CIOF(Iris_a, Iris_b)$.

1: Track all the corners of *vcode* I_A^v in *vcode* I_B^v and that of *hcode* I_A^h in *hcode* I_B^h.
2: Calculate the number of successfully tracked corners in *vcode* tracking (*i.e.* stc_{AB}^v) and *hcode* tracking (*i.e.* stc_{AB}^h) that have their tracked position within TH_d and their local patch dissimilarity under TH_e.
3: Similarly calculate successfully tracked corners of *vcode* I_B^v in *vcode* I_A^v (*i.e.* stc_{BA}^v) as well as *hcode* I_B^h in *hcode* I_A^h (*i.e.* stc_{BA}^h).
4: Quantize optical flow direction for each successfully tracked corners into only eight directions (*i.e.* at $\frac{\pi}{8}$ interval) and obtain 4 histograms $H_{AB}^v, H_{AB}^h, H_{BA}^v$ and H_{BA}^h using $stc_{AB}^v, stc_{AB}^h, stc_{BA}^v$ and stc_{BA}^h respectively.
5: For each histogram, out of 8 bins the bin (*i.e.* direction) having the maximum corners is considered as the consistent optical flow direction. The maximum value obtained from each histogram is termed as corners having consistent optical flow represented as $cof_{AB}^v, cof_{AB}^h, cof_{BA}^v$ and cof_{BA}^h.
6: $ciof_{AB}^v = 1 - \frac{cof_{AB}^v}{N_a^v}$; $ciof_{BA}^v = 1 - \frac{cof_{BA}^v}{N_b^v}$;[Cor. with Inconsis. Opti. Flow (*vcode*)]
7: $ciof_{AB}^h = 1 - \frac{cof_{AB}^h}{N_a^h}$; $ciof_{BA}^h = 1 - \frac{cof_{BA}^h}{N_b^h}$;[Cor. with Inconsis. Opti. Flow (*hcode*)]
8: **return** $CIOF(Iris_a, Iris_b) = \frac{ciof_{AB}^v + ciof_{AB}^h + ciof_{BA}^v + ciof_{BA}^h}{4}$;[SUM RULE]

performance of the proposed system because some of the images are having more discrimination in vertical direction while others have it in horizontal direction. Any corner is considered as tracked successfully if the euclidean distance between itself and its estimated tracked location and the local patch-wise sum of absolute difference is less than TH_d and TH_e respectively. Out of all the successfully tracked corners (stc_{AB}^v, stc_{AB}^h) those that are having inconsistent optical flow are considered as false matches. In order to make measure symmetric the average of $ciof_{AB}$ and $ciof_{BA}$ is used.

3 Experimental Results

Database: The proposed system is tested on two publicly available CASIA V4 Interval and Lamp iris databases. Interval database contains 2,639 iris images collected from 249 subjects having 395 distinct irises and about 7 images per iris. On the other hand Lamp is huge database consisting of 16,212 images collected from 411 subjects having 819 distinct irises and 20 images per iris. Interval images are taken in two session under indoor environment while Lamp images are taken in only one session under indoor environment with lamp on/off. Iris images in Lamp database are more challenging because of nonlinear deformation due to variations of visible illumination. Also, it is a challenge to get good results on any huge database because number of false acceptances grows very fast with the database size [1].

Default parameters								
$Database$	$s(scale)$	t	$p_{r_{min}}$	$p_{r_{max}}$	$i_{r_{min}}$	$i_{r_{max}}$	W	$\alpha_{range}(radians)$
Interval	0.5	0.41	20	90	80	130	15	$(-\pi/4, \pi/6) \cup (5\pi/6, 5\pi/4)$
Lamp	0.5	0.125	16	70	65	120	11	$(-\pi/3, 0) \cup (\pi, 4\pi/3)$

Table 1. Parameters: $p_{r_{min}}$, $p_{r_{max}}$, $i_{r_{min}}$ and $i_{r_{max}}$ are Pupil and Iris radius range

Eyelid	Eyelash	Spec.Reflection	Pupil Noise	Bright image	Dark image
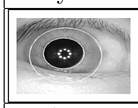	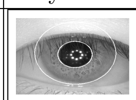	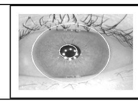	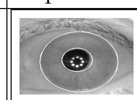	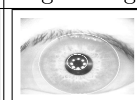	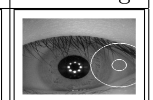
4,300	15,288	5,68	71,160	11,1	39,53

Table 2. Segmentation Error. (Last row: errors occurred in Interval, Lamp databases)

3.1 Segmentation Accuracy

The segmentation accuracy of the proposed system is found to be 94.5% and 94.63% for Interval and Lamp database respectively using the default parameters as shown in Table 1. The erroneous segmentations are critically analyzed and are corrected by adjusting few parameters. This adjustment helps to achieve an accuracy of more than 99.6% on both databases. Some very critically occluded images are segmented manually ($< 0.4\%$). The error analysis along with some of the example images where the proposed segmentation has been failed are shown in Table 2. There are only two critical parameters viz. threshold (t) and angular range (α_{range}) (as defined in Section 2.1) that are required to be adjusted as suggested in Table 3 for accurate segmentation.

Threshold parameter (t) value					Suggested Variation	
Sub-Category	Mean	Min	Max	Std Devi.	(t) value	α_{range}
Eyelid	0.39	0.36	0.41	0.022	-	↓
Eyelash	0.39	0.3	0.43	0.040	↓-	↓
Specular Reflection	0.44	0.36	0.5	0.066	↑	-
Pupil Boundary Noise	0.4	0.26	0.5	0.056	↑↓	-
Bright image	0.46	0.35	0.52	0.06	↑	-
Dark image	0.36	0.25	0.51	0.052	↓	-

Table 3. Statistics and the suggested variations for t and α_{range}

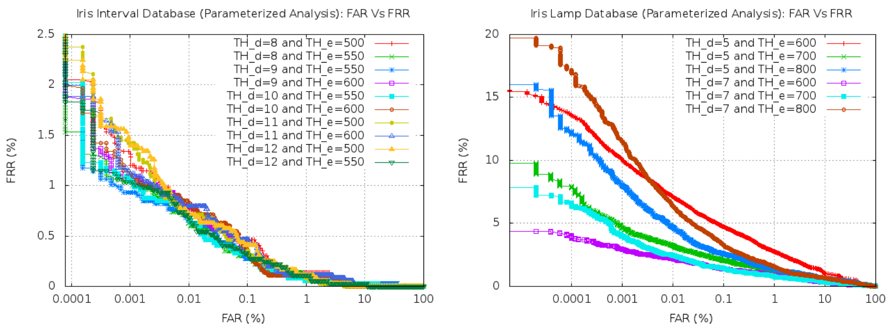

Fig. 5. ROC of proposed system for different set of parameters (only *vcode* matching)

3.2 Recognition Accuracy

This subsection analyses the recognition performance of the proposed system. In all of the graphs *vcode* represents results using only *vcode* matching and similar representation for *hcode* and fusion is used. In order to test the system on Interval database, iris images of first session are taken as training while remaining are taken as testing. For Lamp database, first 10 image are considered as training and rest are taken as testing images. Hence a total of $3,657$ genuine and $1,272,636$ imposter matchings are considered for Interval database testing while $78,300$ genuine and $61,230,600$ imposter matchings are considered for Lamp database. The performance of the system is measured using correct recognition rate (CRR) in case of identification and equal error rate (EER) for verification. The CRR (*i.e.* the **Rank 1** accuracy) of any system is defined as the ratio of the number of correct (Non-False) top best match of iris ROI and the total number of iris ROI in the query set. At any given threshold, the probability of accepting the impostor, known as false acceptance rate (FAR) and probability of rejecting the genuine user known as false rejection rate (FRR) are obtained. Equal error rate (EER) is the value of FAR for which FAR and FRR are equal.

$$EER = \{FAR|FAR = FRR\} \tag{6}$$

Parameterized Analysis: The proposed $CIOF$ dissimilarity measure is primarily parameterized by two parameters TH_e and TH_d. The system is tested using these parameters as input and their values are selected so as to maximize the performance of the system by considering only first 100 subjects from each database and using only *vcode* matching. The parameter values for which system has found to be performing with maximum CRR and minimum ERR are $TH_e = 600$ with patch size of 5×5 and $TH_d = 7$ for Lamp while $TH_e = 600$ with patch size of 5×5 and $TH_d = 10$ for Interval databases as shown in Fig. 5. This parametric analysis inferred that Interval has more translation in iris images of same subject than Lamp database.

Enhancement based Performance Boost-Up: The proposed local enhancement method significantly improves the random micro level iris texture as

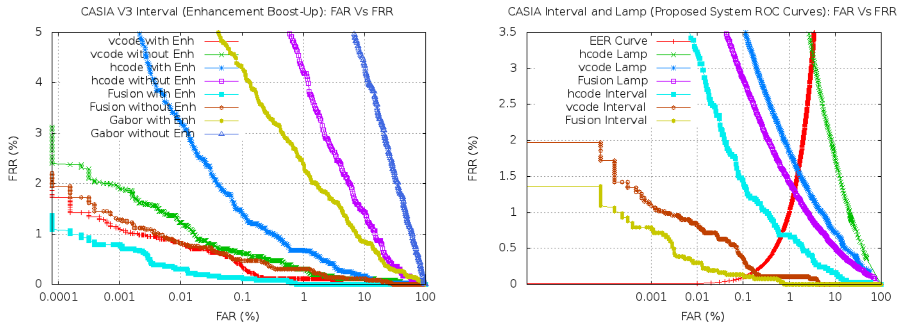

(a) Enhancement based Per. boost-up (b) ROC for Interval and Lamp

Fig. 6. Receiver Operating Characteristic Curves for the Proposed System

Systems	Interval			Lamp		
	DI	CRR%	EER%	DI	CRR%	EER%
Daugman	1.961	99.46	1.881	1.2420	98.90	5.59
Li Ma [19]	-	95.54	2.07	-	-	-
Masek	1.99	99.58	1.09	-	-	-
K. Roy [19]	-	97.21	0.71	-	-	-
Proposed	**2.35**	**99.75**	**0.108**	**2.22**	**99.87**	**1.29**

Table 4. Comparative Performance Analysis

it is evident from the graph shown in Fig. 6(a). For *vcode, hcode*, fusion or even gabor approach [5], the performance of the system is significantly improved after enhancement.

The proposed system has been compared with state of the art iris recognition systems [5, 12, 13, 19]. For comparing with [5, 13] we have coded their systems and with [12, 19] we have used the results as stated in [19]. It is found that the CRR (**Rank 1** accuracy) of the proposed system is more than 99.77% for both databases. The comparison of the proposed system with other state of the art systems is shown in Table 4. Further, its EER is 0.108% for Interval and that for Lamp is 1.29% which is better than the reported systems. For both databases, Receiver Operating Characteristics (ROC) curves are shown in Fig. 6(b) for the proposed system. The ROC curves comparing proposed system with the open source Masek system (Log-Gabor) [13] as well as Daugman system (Gabor) [5] are shown in Fig. 7. Masek's system cannot be tested on Lamp database as the optimal parameters are not known and with default set of parameters its performance is very poor. The decidability index ($d^{'}$) measures separability between imposter and genuine matching scores is defined as:

$$d^{'} = \frac{|\mu_G - \mu_I|}{\sqrt{\frac{\sigma_G^2 + \sigma_I^2}{2}}} \qquad (7)$$

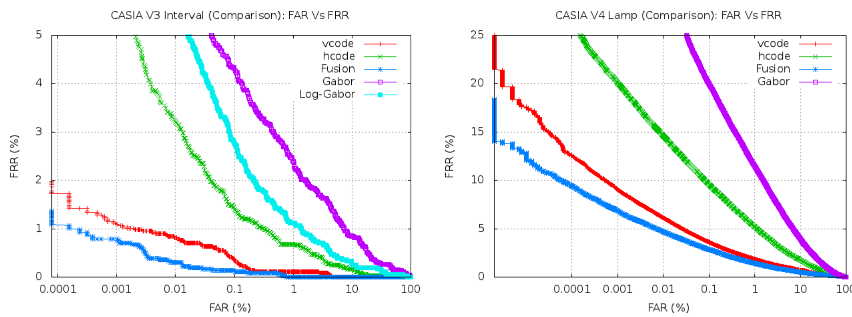

Fig. 7. Comparing Proposed System

where μ_G and μ_I are the mean, and σ_G and σ_I are the standard deviation of the genuine and imposter scores respectively. The decidability index ($d^{'}$) are found to be 2.35 and 2.22 for Interval and Lamp databases respectively.

4 Conclusion

In this paper an efficient iris based authentication system has been proposed. Inner iris boundary is segmented using the improved circular hough transform while outer boundary is detected using integro-differential operator. Texture of the normalized iris images are enhanced using the proposed local enhancement method. The segmented and enhanced iris images are transformed using local gradient binary pattern ($LGBP$) so as to get robust image information representation (*i.e. vcode, hcode*). The corner features are matched using a dissimilarity measure Corners having Inconsistent Optical Flow ($CIOF$) that tracks corners using KL tracking. The proposed system has been tested on publicly available CASIA 4.0 Interval and Lamp databases consisting of $2,639$ and $16,212$ images respectively. The segmentation accuracy of 99.6% has been achieved with little bit of parameter tuning on both databases. The errors in segmentation are classified into six classes and parameterized segmentation analysis is also carried out to infer the influence of parameters towards errors. The system has achieved CRR of 99.75% with an EER of 0.108% on Interval and CRR of 99.87% with an EER of 1.29% on Lamp databases.

References

1. S. C. Amit J. Mhatre, Srinivas Palla and V. Govindaraju. Efficient search and retrieval in biometric databases. *Proc. SPIE*, 5779:265–273, 2005.
2. A. Bendale, A. Nigam, S. Prakash, and P. Gupta. Iris segmentation using improved hough transform. In *International Conference on Intelligent Computing (ICIC)*, pages 408–415, 2012.

3. K. W. Bowyer, K. Hollingsworth, and P. J. Flynn. Image understanding for iris biometrics: A survey. *Computer Vision and Image Understanding*, 110(2):281 – 307, 2008.
4. J. Cui, Y. Wang, J. Huang, T. Tan, and Z. Sun. An iris image synthesis method based on pca and super-resolution. In *Proceedings of the 17th International Conference on Pattern Recognition (ICPR)*, volume 4, pages 471–474. IEEE, 2004.
5. J. Daugman. High confidence visual recognition of persons by a test of statistical independence. *IEEE Transactions on Pattern Analysis and Machine Intelligence*, 1993.
6. J. Daugman. How iris recognition works. In *International Conference on Image Processing (ICIP)*, pages 33–36, 2002.
7. J. Daugman and C. Downing. Epigenetic randomness, complexity and singularity of human iris patterns,. *Proceedings of Royal Society London Biological Sciences*, 2001.
8. R. Farouk. Iris recognition based on elastic graph matching and gabor wavelets. *Computer Vision and Image Understanding*, 115(8):1239 – 1244, 2011.
9. Y. Huang, S. Luo, and E. Chen. An efficient iris recognition system. In *Proceedings of the International Conference on Machine Learning and Cybernetics*, volume 1, pages 450–454. IEEE, 2002.
10. A. Jain, S. Pankanti, S. Prabhakar, L. Hong, and A. Ross. Biometrics: A grand challenge. In *Proceedings of the 17th International Conference on Pattern Recognition (ICPR)*, volume 2, pages 935–942. IEEE, 2004.
11. B. D. Lucas and T. Kanade. An Iterative Image Registration Technique with an Application to Stereo Vision. In *International Joint Conference on Artificial Intelligence (IJCAI)*, pages 674–679, 1981.
12. L. Ma, T. Tan, Y. Wang, and D. Zhang. Efficient iris recognition by characterizing key local variations. *IEEE Transactions on Image Processing*, 13(6):739–750, 2004.
13. L. Masek and P. Kovesi. Matlab source code for a biometric identification system based on iris patterns. *M.Tech Thesis*, 2003.
14. K. Miyazawa, K. Ito, T. Aoki, K. Kobayashi, and H. Nakajima. An effective approach for iris recognition using phase-based image matching. *IEEE Transactions on Pattern Analysis and Machine Intelligence*, 30(10):1741 –1756, oct. 2008.
15. D. Monro, S. Rakshit, and D. Zhang. Dct-based iris recognition. *IEEE Transactions on Pattern Analysis and Machine Intelligence*, 29(4):586 –595, april 2007.
16. A. Nigam and P. Gupta. A new distance measure for face recognition system. In *International Conference on Image and Graphics (ICIG)*, pages 696–701, 2009.
17. A. Nigam and P. Gupta. Comparing human faces using edge weighted dissimilarity measure. In *International Conference on Control, Automation,Robotics and Vision (ICARCV)*, pages 1831–1836, 2010.
18. A. Nigam and P. Gupta. Finger knuckleprint based recognition system using feature tracking. In *Chinese Conference on Biometric Recognition (CCBR)*, pages 125–132, 2011.
19. K. Roy, P. Bhattacharya, and C. Y. Suen. Iris recognition using shape-guided approach and game theory. *Pattern Analysis and Applications*, 14(4):329–348, Nov. 2011.
20. J. Shi and Tomasi. Good features to track. In *Computer Vision and Pattern Recognition*, pages 593–600, 1994.
21. Z. Sun and T. Tan. Ordinal measures for iris recognition. *IEEE Transactions on Pattern Analysis and Machine Intelligence*, 31(12):2211 –2226, dec. 2009.
22. R. Wildes. Iris recognition: an emerging biometric technology. *Proceedings of the IEEE*, 85(9):1348–1363, 1997.